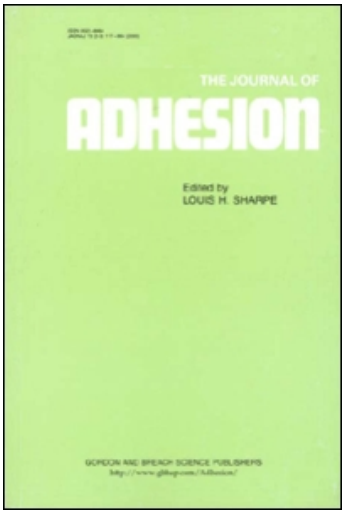

The Journal of Adhesion
Publication details, including instructions for authors and subscription information:
http://www.informaworld.com/smpp/title~content=t713453635

Digital In-Line Holography as a Three-Dimensional Tool to Study Motile Marine Organisms During Their Exploration of Surfaces

M. Heydt[a]; A. Rosenhahn[a]; M. Grunze[a]; M. Pettitt[b]; M. E. Callow[b]; J. A. Callow[b]
[a] Angewandte Physikalische Chemie, Universität Heidelberg, Heidelberg, Germany [b] School of Biosciences, University of Birmingham, Birmingham, U.K.

To cite this Article Heydt, M. , Rosenhahn, A. , Grunze, M. , Pettitt, M. , Callow, M. E. and Callow, J. A.(2007) 'Digital In-Line Holography as a Three-Dimensional Tool to Study Motile Marine Organisms During Their Exploration of Surfaces', The Journal of Adhesion, 83: 5, 417 — 430
To link to this Article: DOI: 10.1080/00218460701377388
URL: http://dx.doi.org/10.1080/00218460701377388

The Journal of Adhesion, 83:417–430, 2007

ISSN: 0021-8464 print/1545-5823 online
DOI: 10.1080/00218460701377388

Taylor & Francis
Taylor & Francis Group

Digital In-line Holography as a Three-Dimensional Tool to Study Motile Marine Organisms During Their Exploration of Surfaces

M. Heydt
A. Rosenhahn
M. Grunze
Angewandte Physikalische Chemie, Universität Heidelberg, Heidelberg, Germany

M. Pettitt
M. E. Callow
J. A. Callow
School of Biosciences, University of Birmingham, Birmingham, U.K.

The swimming patterns of zoospores of the green alga Ulva linza *in the vicinity of a surface were investigated by digital in-line holography. Full 3D motion patterns were retrieved from measurements and the traces obtained were compared with known swimming patterns of spores of the brown alga* Hincksia irregularis *and the green alga* Ulva linza *as seen in a conventional optical microscope. Quantitative information such as swimming velocity was calculated from the 3D traces. The results demonstrate the potential of digital in-line holography to image and quantify exploratory patterns of behavior of motile spores close to surfaces. This technique can give detailed insight into mechanisms of surface colonization by spores and larvae of fouling organisms in response to changes in surface properties.*

Keywords: Biofouling; Digital in-line holography; Exploration pattern; Gabor; Surface exploration; Three-dimensional tracking; *Ulva linza*

Received 15 November 2006; in final form 6 March 2007.
One of a Collection of papers honoring Liliane Léger, the recipient in February 2007 of The Adhesion Society Award for Excellence in Adhesion Science, Sponsored by 3M.
Address correspondence to Matthias Heydt, Angewandte Physikalische Chemie, Universität Heidelberg, INF 253, D-69120, Heidelberg, Germany.
E-mail: m.heydt@urz.uni-heidelberg.de

INTRODUCTION

Many sessile marine organisms reproduce by the production of motile spores or larvae. For such organisms, locating and settling on a surface is a critical stage in their life cycle. Because of the importance of this step for survival and reproduction, surface colonization is not a random process, and there is a substantial body of evidence that shows it is moderated by the chemical and physical nature of the surface [1,2]. When the surface colonized by these organisms is a manmade structure such as the hull of a vessel, the settlement of spores or larvae contributes to biofouling. One of the key ideas for the development of novel antifouling coatings is to exploit the choosiness of the settling (adhesion) stages of fouling organisms by creating a deterrent surface [1–3]. It has been shown that the exploration of surfaces, *e.g.*, by the cypris larva of the tropical barnacle *Balanus amphitrite*, involves distinct motion patterns that depend on the properties of the surface [4]. The exploration behavior of spores of the brown alga *Hincksia irregularis* was also investigated by compound microscopy [5]. Five different swimming patterns (straight path, search circles, orientation, gyration, and wobbling) were distinguished, facilitating a new antifouling bioassay by determining the change in the ratio of RCD (rate of change direction) and SPD (swimming speed) [6–8]. By introducing certain chemicals into seawater, the ratio of RCD/SPD changed. The swimming and surface exploration behaviors of *Ulva* spores, which are addressed in this article, have been studied before by video microscopy [9]. A transition from an erratic, random motion followed by a more localized searching pattern was observed prior to settlement. The final settlement stage involves a rapid spinning motion on the substratum, immediately prior to the irreversible commitment to settlement and secretion of adhesive. However, the three-dimensionality of the motion of a swimming algal spore makes it difficult for conventional optical microscopy to follow the cell throughout its exploration phase from a point far away from the surface to the close vicinity of the surface where sensing occurs. High-speed data acquisition in modern light microscopes allows algal cells to be traced, but the intrinsic two-dimensionality of the technique provides only either the projection of the trace (large depth of focus) or the visualization of one focal plane (small depth of focus). In general, a quantification of motion is difficult with this type of compound microscopy as all three-dimensional coordinates are mandatory to perform an accurate calculation of, for example, swimming velocity. In this article, we demonstrate the feasibility of digital in-line holography as an intrinsically three-dimensional microscopy technique to investigate surface exploration behavior of zoospores of the green alga *Ulva linza*. Sample traces obtained during exploration and early settlement stages are shown.

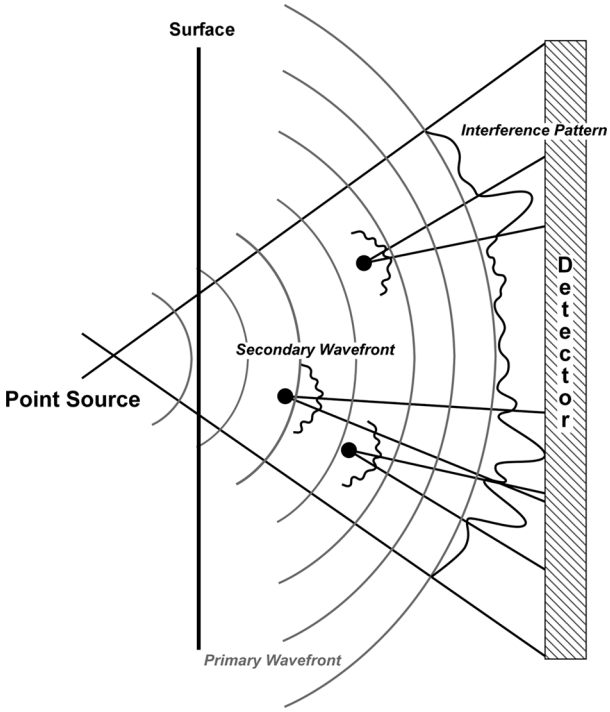

FIGURE 1 General principle of digital in-line holography and pattern formation for a moving particle such as a zoospore of the alga *Ulva*.

The basic idea of in-line holography was first described by Gabor [10] in 1948. The underlying concept is the formation of a diffraction pattern when coherent radiation is penetrating a sample. As shown in Fig. 1, the undisturbed photons ("primary wavefront" or "reference wave") and those scattered from the object ("secondary wavefront") interfere and form the observed diffraction pattern. From this so-called hologram, real space information can be retrieved either optically or digitally by a reconstruction algorithm [11]. In principle, in-line holography can be carried out with parallel or spherical wavefronts. Parallel wavefronts are easier to handle, and the reconstruction algorithms are easier to implement. If digital detectors are used, the trade-off is the limitation of the resolution by the size of the pixels. Such a parallel wavefront approach has been implemented successfully for a variety of questions that are relevant for our underwater research studies [12]. The limitation of the resolution by the pixel spacing was, on the one hand, overcome by using conventional photographic plates, which, on the other hand, are limited in terms of acquisition frequency

and total number of images. Nonetheless, the advantage of using holography for underwater research is obvious for the investigation of large volumes because there is no necessity for focusing, as this can be done later using the computer. If spherical wavefronts are used for holography, the resolution is no longer limited by the pixel size of the detector, but by the wavelength and acceptance angle of the detector system [11,13]. Furthermore, if oil-immersion techniques are applied, holographic microscopy is possible with high magnification and at a resolution of less than a micrometer [14]. Digital in-line holography is especially powerful in tracking objects by a combination of multiple exposures [15]. As has been shown in microfluidic experiments [16] and the tracking of the unicellular alga *Tetraselmis* and bacteria [17], moving objects can be followed in three dimensions with remarkable accuracy and high time resolution. Applications such as the determination of the swimming speed of the alga *Alexandrium* (Dinophyceae) show that scientific questions about swimming behavior of certain marine species can be addressed by this technique [18]. A major advantage is the application of digital in-line holographic microscopy (DIHM) in the field as some measurements were performed with a device deployed in the ocean up to a depth of 20 m [12,19]. The technique can be applied to an environment where it is mostly impossible to use a conventional microscope. However, the technique has not yet been applied to studies of swimming organisms that show surface exploration and settlement/adhesion types of behavior. In this article, we show the applicability of digital in-line holography to study the surface exploration behavior of zoospores of the green alga *Ulva linza*. A glass surface was used because this is the most commonly used standard surface for experiments and observations on *Ulva* spore settlement and adhesion [9].

Ulva, syn *Enteromorpha*, is a common, green macroalga found throughout the world in the upper intertidal zone of seashores and as a fouling organism on a variety of manmade structures including ships' hulls [20]. Like the dispersal stages of other sessile marine organisms, *Ulva* zoospores need to locate and adhere to a surface quickly to complete their life history. Once a zoospore has located a suitable surface, it goes through a process of settlement whereby the motile cell becomes anchored to the surface through the release of a glycoprotein adhesive [3]. The whole process of settlement and adhesion can occur within seconds to minutes of presenting a suitable surface to a population of spores. Like the two-dimensional studies mentioned previously information about the exploration of surfaces by zoospores prior to settlement will provide important insight into the sensing mechanism of this class of marine organisms. Such information is relevant to the design of novel antifouling coatings for marine environments.

MATERIALS AND METHODS

Experimental Setup

The underwater holographic microscope is similar to the setup described previously [19] and was purchased from Helix Science Application [21]. In addition, a sample stage was implemented in the microscope to mount a coverslip or a microscope slide at a defined position. A new observation chamber was also constructed to work with a defined volume. Even though it is possible to use this device underwater, for more controlled conditions in which to test the applicability of this device to settling organisms, all current experiments were performed on a laboratory bench without submersing the whole microscope.

The surfaces used for zoospore settlement were glass coverslips (22 mm × 50 mm) cleaned in 0.1 M HCl solution for 24 h and rinsed extensively in deionized water.

Ulva Zoospore Suspensions

Fertile plants of *Ulva linza* were collected from the seashore at Llantwit Major, South Wales, U.K. (51°40′ N; 3°48′ W) in September 2006, 4 days before the full moon. Zoospores were released and prepared for settlement studies as described previously [9]. The observation chamber of the holographic microscope was filled with 100 ml of 0.2-μm-filtered artificial seawater, and 200 μl of a spore suspension containing 1.5×10^6 spores ml^{-1} solution were added, giving a final concentration of 3×10^3 spores ml^{-1}. Swimming behavior in the vicinity of a glass coverslip was studied over 1 h. A set of 200 holograms was recorded with an acquisition frequency of 11 frames per second. The holograms were stored and analyzed later by the algorithms described later.

Reconstruction and Analysis

The experiment analyzed in this study consisted of 200 sequential holograms. For each hologram, a full three-dimensional reconstruction was necessary, and each hologram was analyzed in 16 z planes to determine the accurate z position of any spore. The amount of data analyzed was 3200 images or 3.125 GB of data.

All reconstructions of the holograms were performed with the DIHM software package purchased from Helix Science Application [21], which is based on the Kreuzer-patented implementation of the Kirchhoff–Helmholtz transformation [15]. The basic principle for composite holograms and tracking was described previously [15,16]. The three-dimensional trace analysis was carried out with new custom-designed

software routines to find the accurate x,y, and z position mostly automatically. To determine a projected lateral path, all z layers of one frame were added up into a single image. In all sum images, the x,y position of the spore was determined manually. This crude x,y position was refined automatically by a main focus determination. Using this precise x, y position for any spore in each frame, the z position was also determined automatically by main focus determination in the corresponding z layers.

Because of the intrinsic divergence of the illumination, the analyzed field of view changed constantly throughout different z distances between the pinhole and the object. At a distance of 1100 μm from the pinhole, the field of view was $363 \times 363\,\mu m^2$, and at 2100 μm above the pinhole, the field of view was $693 \times 693\,\mu m^2$. With the field of view, the magnification also changes through the investigated volume. Close to the surface, the field of view was $419 \times 419\,\mu m^2$, which corresponds to a magnification of 460. The error of the position determination was tested by changing the trace starting values and running the algorithm again. The positions obtained were compared to confirm the self-consistency of the algorithm. A detailed error determination on position determination in holography is currently being developed. The error, *e.g.*, for the x,y position for the described experiment, was determined to be $\pm 0.1\,\mu m$. For all described motion patterns, quantitative values are given, *e.g.*, for the velocity. However, before generalizing the absolute values, more data are necessary.

RESULTS AND DISCUSSION

Figure 2a shows a part of a typical hologram sequence that was recorded over a time period of approximately 20 s. Out of the whole series, 50 frames recorded at a rate of 11 frames per second were added up according to the algorithm described previously [15]. The reconstruction algorithm described previously can be applied to the hologram for different reconstruction planes, and sections through the observation volume can be retrieved. Figures 2b and 2c show two of those reconstruction planes. Hence, from the same hologram sequence, spores at different depths in the volume of seawater can be reconstructed at a time. To obtain the best depth resolution in the three-dimensional position optimization, only two frames were accumulated and reconstructed. As described before, for each position of the spores, a complete stack of images throughout the volume was reconstructed and the precise position of every spore at a different time point was determined. As result, a set of x, y, z coordinates for one spore as a function of time can be extracted from the scattering

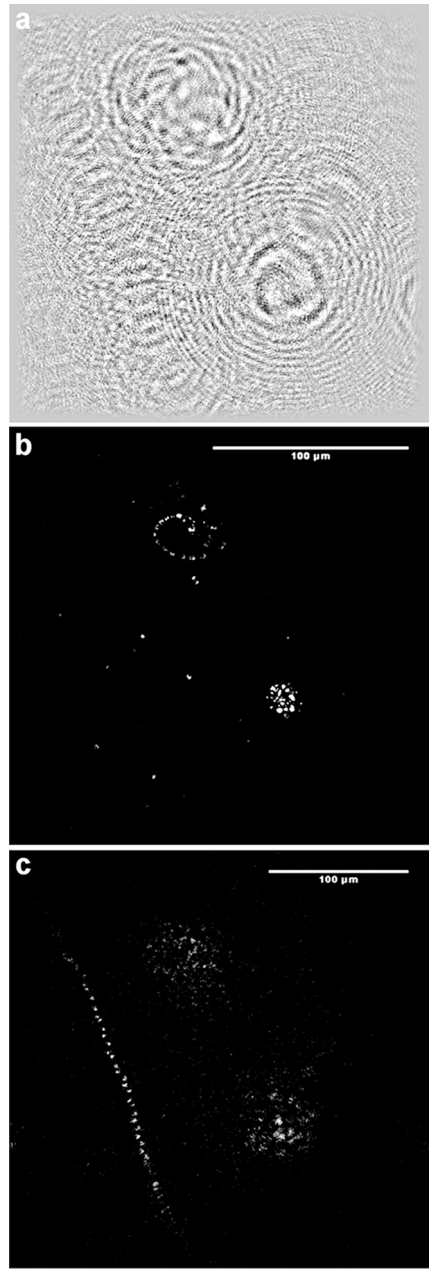

FIGURE 2 Recorded hologram series and reconstructed images; a) accumulated hologram consisting of 50 single frames, b) reconstruction of hologram (a) 1300 µm above the pinhole, and c) reconstruction of hologram (a) 1830 µm above the pinhole.

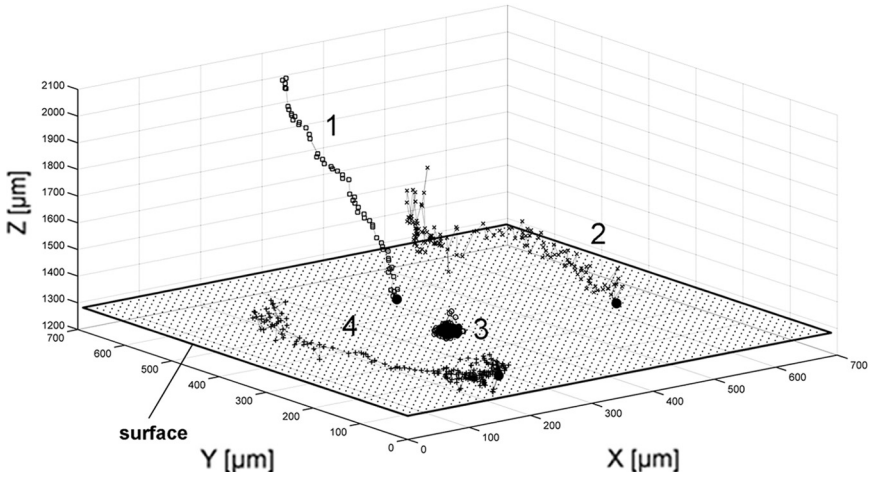

FIGURE 3 Three-dimensional swimming pattern determined from the hologram series for four different spores observed simultaneously within the observation volume. All four traces start at the position of the slightly larger black dot.

patterns. Such a four-dimensional matrix was calculated for each spore that swam through the observation volume during the measurement. Note that both the interaction between different spores and their interaction with the surface can be followed simultaneously.

Although the picture stacks retrieved from the hologram comprise a large amount of data, the extraction of the four-dimensional matrices as described previously is mandatory to represent and quantify the motion in an effective manner. Figure 3 shows one of the three-dimensional plots of the movement of four (labeled 1–4) different *Ulva* spores. The data were retrieved from the single hologram series shown in Figure 2a, *i.e.*, the four different swimming patterns labeled 1–4, were observed simultaneously in the same time interval. From this three-dimensional plot, it becomes obvious that the four spores behave differently. Although spore 3 found a suitable place on the surface to settle, spores 1 and 2 were swimming at a certain distance from the surface without noticeable interaction. Spore 4 resembles an intermediate state; the spore is seen to explore the surface by attaching, then moving in close proximity to the surface and detaching. This behavior becomes clearer looking at the projections of the motion in Figure 4. Figure 4a shows the lateral position projected down onto the surface (top view) and Figure 4b the side view of the swimming depth. While the projection shows the exploratory patterns on the

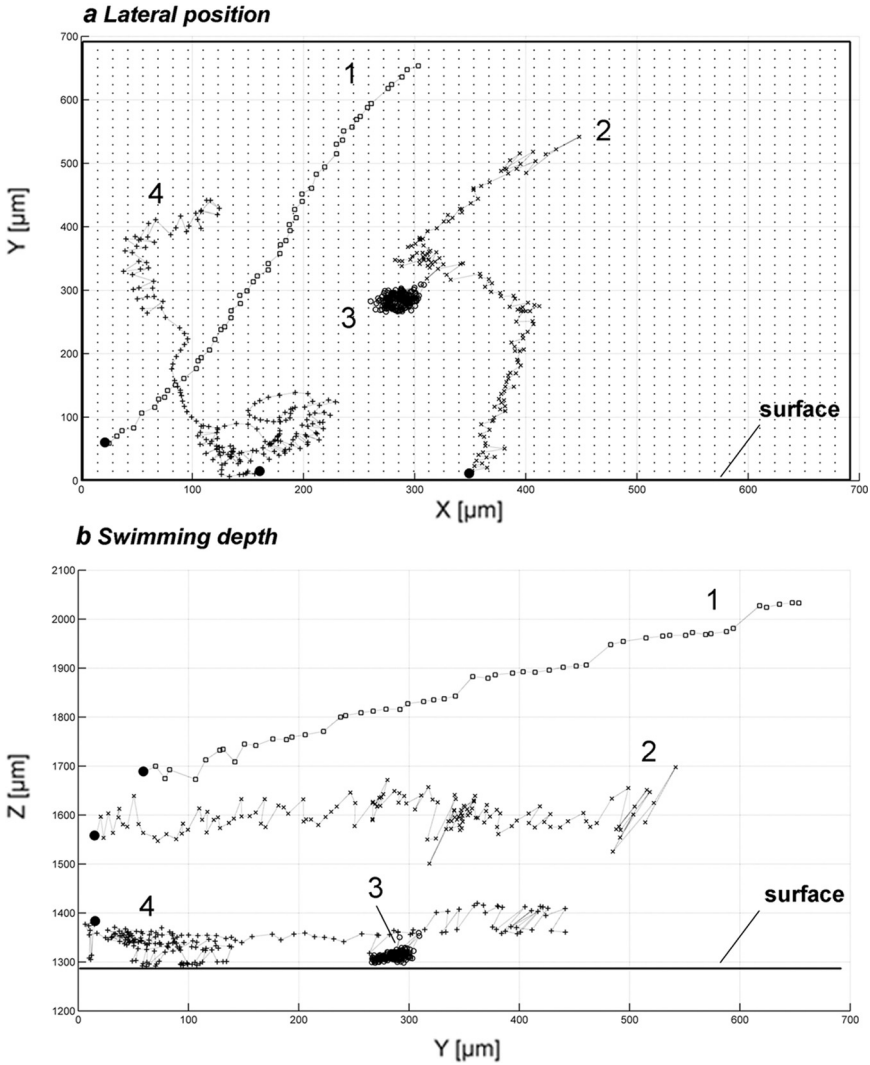

FIGURE 4 Two-dimensional projections of the trace shown in Figure 3: a) lateral view of the swimming pattern and b) swimming depth during the swimming pattern.

surface ("exploration logic"), the diving depth in projection reveals if the spore is in contact with the surface. With the information in Figures 3 and 4, we can now qualitatively assign the observed swimming patterns to the classification used by Iken *et al.* [5]. Five different

patterns of motion, (1) straight path, (2) gyration, (3) search circle, (4) orientation, and (5) wobbling, were distinguished. Although this assignment was given for spores of a different alga, namely *Hincksia irregularis*, this concept obviously is also applicable to spores of *Ulva*. However, the search cycles for *Hincksia* spores are much bigger than for *Ulva* spores, and the wobbling pattern could not be found in the experiment reported here.

Pattern 1 is assigned to what is known as a straight path in the case of brown algae *Hincksia irregularis* [5]. In our experiments, this movement only occurred far away from the surface (Figure 4b), which is in agreement with the qualitative observations reported in Ref. [5]. The suggestion that the spore uses this motion to move over a large distance and not to search a place to settle seems reasonable. From the data, we can also derive quantitative information such as the mean swimming distance between two frames ($18\,\mu m \pm 21\,\mu m$) or the average swimming speed ($302\,\mu m \cdot s^{-1} \pm 236\,\mu m \cdot s^{-1}$). In contrast to the two-dimensional investigations using a compound microscope, all three dimensions determined contribute to the velocity calculation as the three-dimensional distance vector $\Delta\vec{d}$ between two subsequent positions i and j results in $\Delta\vec{d} = \vec{d}_i - \vec{d}_j$. Each of the position vectors $\vec{d}_i$ and $\vec{d}_j$ consist of x, y, and z coordinates. The velocity was obtained by calculating the absolute of this vector divided by the time between the two pictures: $\nu = |\Delta\vec{d}|/\Delta t$. Pattern 2 shows what is for brown algae known as orientation [5] or is described for *Ulva linza* as erratic, random motion [9]. In this pattern, the spore changes its direction of swimming with high frequency. The spore is relatively close to the surface, but it is not known whether the spore recognizes the surface such that it has an effect on its motion. The mean swimming distance per frame was $30\,\mu m \pm 24\,\mu m$, and the average swimming speed as determined from this trace was $334\,\mu m\,s^{-1} \pm 269\,\mu m\,s^{-1}$. The velocity values for pattern 2 were similar to those observed in pattern 1, but the standard deviation in pattern 2 was higher because of the frequent changes in the direction of movement.

In the following, we concentrate on traces 3 and 4, which are relevant to find out if there is an exploratory logic in the motion of *Ulva* spores. Pattern 3, known as search circle [5], is represented in a magnified top view in Figure 5. This behavior is a typical motion for spores in the direct vicinity of the surface at what appears to be a hospitable position. In this pattern, the spore was always in contact with the surface and appears to test the surface for a relatively long period of time while swimming frequently over the same area. Obviously, the swimming distance between different frames is much smaller ($17\,\mu m \pm 6\,\mu m$) than in the case of traces 1 and 2. The average speed

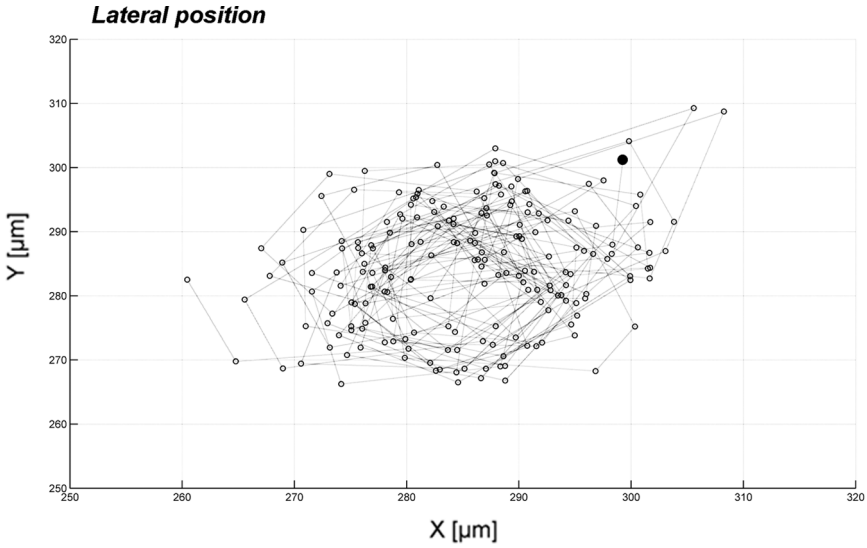

FIGURE 5 Detail top view of search pattern 1 from Figure 3.

was $188\,\mu m \cdot s^{-1} \pm 74\,\mu m \cdot s^{-1}$. The probed surface area during the observation time of 20 s was $50 \times 50\,\mu m^2$.

Although pattern 3 shows a spore that almost settled on a certain spot and searched within a very restricted area, pattern 4 resembles an interaction pattern that is between patterns 1 or 2 and pattern 3. The spore in pattern 4 changes between a straight-path motion and an explorative behavior with some touchdowns on the surface. This intermediate behavior is described as gyration [5] and appears to be similar to the change from erratic random motion into a more localized searching behavior previously reported for *Ulva* spores [9]. This pattern is very important for understanding the sensing abilities of a zoospore. It seems only to occur at a certain distance above the surface where the spore swims over the surface and touches or senses the surface occasionally, trying to find a place that is worth exploring in more detail. If the spore decides to descend onto the surface, the swimming pattern changes into the search circle motion (*cf.* pattern 3). The gyration pattern can be divided into different phases (Figure 6): in the beginning (part A) of the trace, the organism moves in circles over the surface with occasional touchdowns. Eventually (part B), the zoospore moves in a straight path over the surface to attempt a different spot. In this case, the organism starts probing the surface only for a very short time (part C), but long enough to decide whether to continue

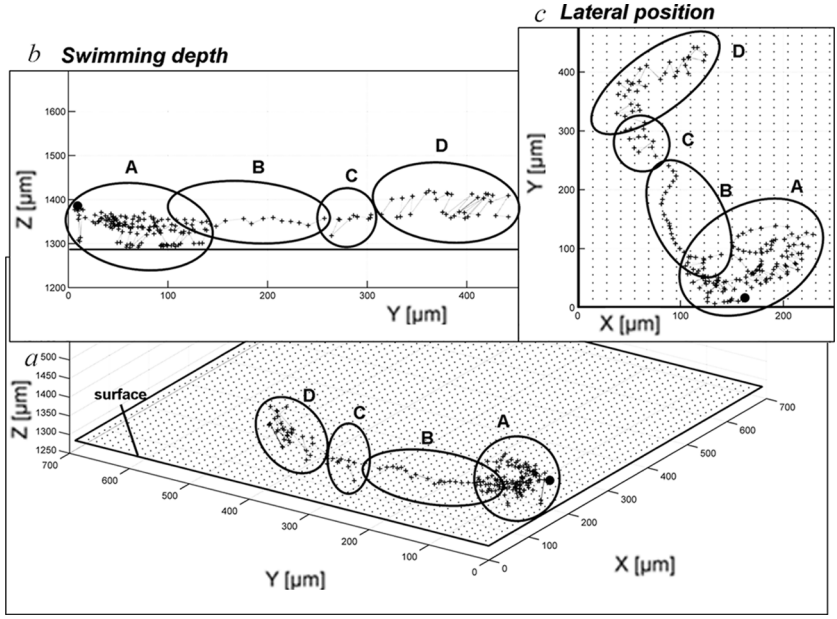

FIGURE 6 Different motion patterns A–D during the gyrational motion of trace 4: a) three-dimensional view of the trace, b) swimming depth, and c) lateral view of the swimming pattern.

with an orientation motion similar to pattern 2 (part D). The swimming properties during this observation time can be quantified. The intermediate motion (parts A, B, C, and D) had a mean swimming distance per frame of $19\,\mu m \pm 17\,\mu m$, and the average speed was $215\,\mu m \cdot s^{-1} \pm 151\,\mu m \cdot s^{-1}$. During the gyration pattern in parts A, B, and C, the spore was located at $80 \pm 20\,\mu m$ above the surface. In part A of the pattern, the total area in which the spore was probing the surface was $150 \times 150\,\mu m^2$. For probing this surface area, which is six times as large as the probed area of the spore in pattern 3, the spore spends less time (~ 5 s) than the spore of pattern 3. This highlights the difference between these two patterns. The mean swimming distance per frame for part A is $17\,\mu m \pm 11\,\mu m$, and the average speed observed is $189\,\mu m \cdot s^{-1} \pm 127\,\mu m \cdot s^{-1}$. Both values are significantly larger than in pattern 3 and smaller than in pattern 1 or 2. This indicates that the gyration state is a real intermediate state between intensive searching and free swimming. In Part D of the gyration pattern, the mean swimming distance per frame ($30\,\mu m \pm 17\,\mu m$) and the average speed ($329\,\mu m \cdot s^{-1} \pm 189\,\mu m \cdot s^{-1}$) increases to a value similar

to pattern 1 or 2. This measurement shows the change from the gyration pattern to the orientation pattern, which is accomplished by the increase of velocity.

CONCLUSION

We have demonstrated the applicability of digital in-line holography to answer questions relevant to understanding how *Ulva* zoospores explore surfaces. Such patterns are relevant to understanding how surface properties may moderate exploration and aid in the development of antifouling coatings. Full three-dimensional motion patterns were retrieved from the measurements and identified as specific motion patterns. Quantitative information such as the velocity in a specific motion pattern was calculated. However, without more data and, hence, better statistics, we cannot yet generalize these results. In future work, exploration patterns of *Ulva* zoospores will be studied on surfaces with different surface properties, *e.g.*, topography and chemistry. The goal is to find a correlation between surface properties (energy, chemistry, morphology, charge, and mechanical properties) and the exploration behavior of zoospores leading to settlement and permanent adhesion.

ACKNOWLEDGMENTS

The work was funded by the EC Framework 6 Integrated Project AMBIO (Advanced Nanostructured Surfaces for the Control of Biofouling). This article reflects only the authors' views, and the European Community is not liable for any use that may be made of information contained therein. A. R. acknowledges the Fonds der Chemischen Industrie for a Liebig research grant and the Landesstiftung Baden-Württemberg for support within the Eliteförderprogramm. For support and stimulating discussions, we thank S. K. Jericho, M. H. Jericho, and H. J. Kreuzer from Dalhousie University, Halifax, Canada.

REFERENCES

[1] Carman, M. L., Estes, T. G., Feinberg, A. W., Schumacher, J. F., Wilkerson, W., and Wilson, L. H., *Biofouling* **22**, 11–21 (2006).
[2] Callow, J. A. and Callow, M. E., *Biofilms* (Springer-Verlag, Berlin, 2006), 1st ed., Chap. 6, pp. 141–169.
[3] Callow, J. A. and Callow, M. E., *Biological Adhesives* (Springer-Verlag, Berlin, 2006), 1st ed., Chap. 4, pp. 63–78.

[4] Marechal, J.-P., Hellio, C., Sebire, M., and Clare, A. S., *Biofouling* **20**, 211–217 (2004).
[5] Iken, K., Amsler, C. D., Greer, S. P., and McClintock, J. B., *Phycologia* **40**, 359–366 (2001).
[6] Iken, K., Greer, S. P., Amsler, C. D., and McClintock, J. B., *Biofouling* **19**, 327–334 (2003).
[7] Greer, S. P., Iken, K., McClintock, J. B., and Amsler, C. D., *Biofouling* **22**, 125–132 (2006).
[8] Amsler, C. D. and Fairhead, V. A., *Adv. Bot. Res.* **43**, 1–91 (2006).
[9] Callow, M. E., Callow, J. A., Pickett-Heaps, J., and Wetherbee, R., *J. Phycol.* **33**, 938–947 (1997).
[10] Gabor, D., *Nature* **161**, 777–778 (1948).
[11] Xu, W., Jericho, M. H., Meinertzhagen, I. A., and Kreuzer, H. J., *Proc. Natl. Acad. Sci. U.S.A.* **98**, 11301–11305 (2001).
[12] Watson, J., Alexander, S., Craig, G., Hendry, D. C., Hobson, P. R., Lampitt, R. S., Marteau, J. M., Nareid, H., Player, M. A., Saw, K., and Tipping, K., *Meas. Sci. Technol.* **12**, L9–L15 (2001).
[13] Kreuzer, H. J., US Patent 6,411,406, June 25, 2002.
[14] Garcia-Sucerquia, J., Xu, W., Jericho, M. H., and Kreuzer, H. J., *Opt. Lett.* **31**, 1211–1213 (2006).
[15] Kreuzer, H. J. and Jericho, M. H., US Patent 2004-069903A1, September 2, 2004.
[16] Garcia-Sucerquia, J., Xu, W., Jericho, S. K., Klages, P., Jericho, M. H., and Kreuzer, H. J., *Appl. Opt.* **45**, 846–850 (2006).
[17] Xu, W., Jericho, M. H., Kreuzer, H. J., and Meinertzhagen, I. A., *Opt. Lett.* **28**, 164–166 (2003).
[18] Lewis, N. I., Xu, W., Jericho, S. K., Kreuzer, H. J., Jericho, M., H., and Cembella, A. D., *Phycologia* **45**, 61–70 (2006).
[19] Jericho, S. K., Garcia-Sucerquia, J., Xu, W., Jericho, M. H., and Kreuzer, H. J., *Rev. Sci. Instrum.* **77**, 043706-1–043706-10 (2006).
[20] Callow, M. E., *Biodeterioration Abstr.* **10**, 411–421 (1996).
[21] Helix Science Applications, Halifax, Nova Scotia, Canada.